

Two Different Approaches to the Fabrication of Nano-Sized Particles in Thick Polyimide Films

Junro Yoon,¹ Dong Joo Choi,¹ Kyu-Hyung Lee,² Jeong Yong Lee,² and Young-Ho Kim^{1,*}

¹Division of Materials Science and Engineering, College of Engineering, Hanyang University, 17 Haengdang-dong, Seongdong-Ku, Seoul 133-791, Korea

²Department of Materials Science and Engineering, Korea Advanced Institute of Science and Technology, Daejeon 305-701, Korea

Relatively thick polyimide films (> 800 nm) containing copper-based nanoparticles were fabricated via two different methods: a multiple-stacking method and a concentrated polyamic acid (PAA) method. For the multiple-stacking samples, we repeated the stacking of 2.5 wt% PAA and 4 nm thick Cu thin film structures and then thermally cured the stacked samples. In the case of the concentrated PAA samples, the concentrated PAA (10 wt%) was spin-coated on the 10 nm and 25 nm thick Cu thin films and thermally cured. The phase and distribution of nanoparticles fabricated by both methods were characterized by X-ray diffraction and transmission electron microscopy. The fabricated nanoparticles were dispersed in thick polyimide films and the size of the nanoparticles was sensitive to the amount of metal sources. The nanoparticles dispersed in the thick polyimide film had two different phases: the metallic copper phase and the cuprous oxide phase. Enhanced surface plasmon resonance absorption was observed in the metallic Cu nanoparticles.

Keywords: nanoparticles, Cu₂O, Cu, polyimide, nanoparticle fabrication, multiple-stacking

1. INTRODUCTION

Metallic or semiconductor nanoparticles dispersed in films have been of interest because of the way their distinctive electrical and optical properties depend on their size.^[1] Polymer films have attracted attention in the engineering field because of their low cost, which makes them easy to fabricate, and their flexible nature, which means that can be applied to various types of products such as optoelectronic thin film and optical amplifier fiber for telecommunication.^[2,3] Nanocomposite films that contain nanoparticles have been developed by several techniques such as electron-beam lithography^[4] and self-assembly.^[5,6] Recently, we reported a simple and novel method of fabricating various types of nanoparticles in a thin polyimide (PI) film (< 100 nm).^[7,8] However, because nanoparticles embedded in a very thin film show low optical absorption and photoluminescence properties, practical optoelectrical applications may be limited.

The dispersion of nanoparticles in thick polymer films (> 800 nm) can be achieved with two possible fabrication methods: the concentrated polymer method and the multiple-stacking method (with layer-by-layer assembly).^[9,10] In the concentrated polymer method, a thick PI film is fabricated by using a high concentration PI precursor. In the other

method, multiple-stacking is used to stack the polyamic acid (PAA)/metal thin film structure in a layer-by-layer assembly. For this paper, we applied both these methods to fabricate copper (Cu)-based nanoparticles dispersed in a relatively thick (> 800 nm) PI film. Our aim is to improve the properties of thin PI film via two different fabrication methods: the multiple-stacking method and the concentrated PAA method. We also discuss the properties of nanoparticles fabricated by means of both fabrication methods.

2. EXPERIMENTAL PROCEDURE

Oxidized silicon and glass substrates were used in this study. Cu thin films were deposited on the substrates by means of a thermal evaporation method. In addition, metal Cu foils and direct current magnetron sputtered substrates were used to confirm the formation of nanoparticles from an unlimited metal source with a high concentration of PAA. The PAA used in this study was the p-phenylene bi-phenyl-tetra-carboximide (BPDA-PDA) type dissolved in N-methyl-2-pyrrolidinone (NMP) from HD MicrosystemsTM, (PI2610). For the multiple-stacking method samples, we stacked PAA/Cu thin film structures by using a layer-by-layer assembly. The deposited 4 nm thick Cu thin film was reacted with spin-coated 2.5 wt% PAA. The samples were soft-baked to evaporate the residual NMP solvent; the evaporated Cu layers

*Corresponding author: kimyh@hanyang.ac.kr

and 2.5 wt% of the PAA layers were then alternately stacked; and the final thickness of the samples was controlled through the number of stacked layers. The stacked samples were thermally cured at 350°C for 2 h in 100 standard cubic centimeters per minute (sccm) and 1000 sccm flow rates of high purity nitrogen atmosphere to imidize the PAA to PI. For the concentrated PAA method, we deposited 10 nm or 25 nm of Cu thin film on the substrates. We then spin-coated 10 wt% PAA on the Cu thin film. The samples were soft-baked after an optimal reaction time. After that, we thermally cured the samples at 350°C for 2 h in a 100 sccm flow rate of high purity nitrogen atmosphere.

3. MULTIPLE-STACKING METHOD

Figure 1 shows cross-sectional transmission electron microscope (TEM) images of nanoparticles in a 10-layer stacked PI films after thermal curing at 100 sccm of a nitrogen gas flow rate. As you see in Fig. 1(a), the fabricated nanoparti-

cles are dispersed in 850 nm thick PI film, and the diameter of the nanoparticles ranges between 20 nm and 28 nm. As shown in Fig. 1(b), the nanoparticles seem to have a core-shell structure. Furthermore, as shown in Fig. 2, the sample cured at 1000 sccm of the nitrogen gas flow rate shows the same distribution as the sample cured with 100 sccm. The fabricated nanoparticles, as shown in Fig. 2(a), were dispersed in 1300 nm thick PI film, though the size of the nanoparticles is smaller than the sample with 100 sccm. In Fig. 2(b), the nanoparticles cured at 1000 sccm vary in size, depending on their positions in PI film; in contrast, the sample cured at 100 sccm contains particles of a relatively uniform size.

To identify how the phase and structure of the nanoparticles depend on their positions, we used high resolution TEM (HRTEM) to characterize the nanoparticles in the top, middle, and bottom regions of a PI film. The obtained HRTEM images were simulated to get Fourier transformation results and spot patterns. From the analysis of the spot patterns, we can get crystallographic information of the nanoparticles in

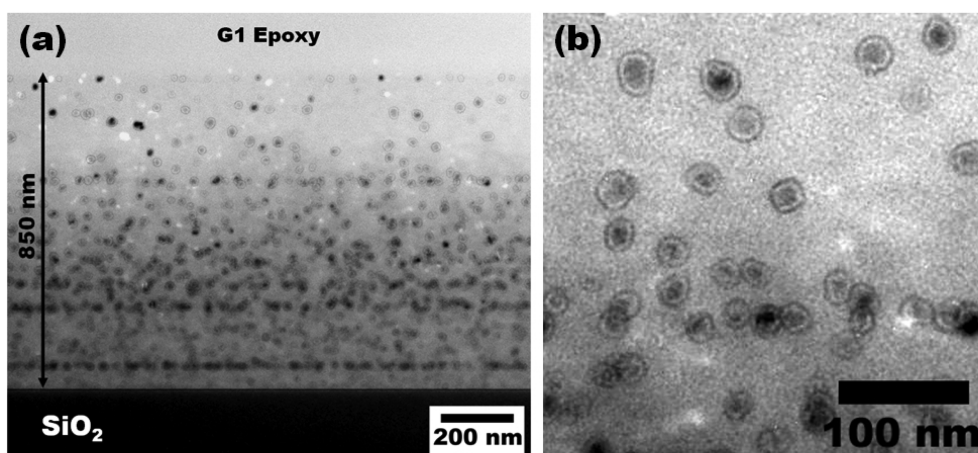


Fig. 1. Cross-sectional TEM images of Cu-Based nanoparticles in multiple-stacked PI films cured at 350°C for 2 h with a 100 sccm N₂ gas flow rate: (a) entire 850 nm thick image and (b) a magnified image of the nanoparticles.

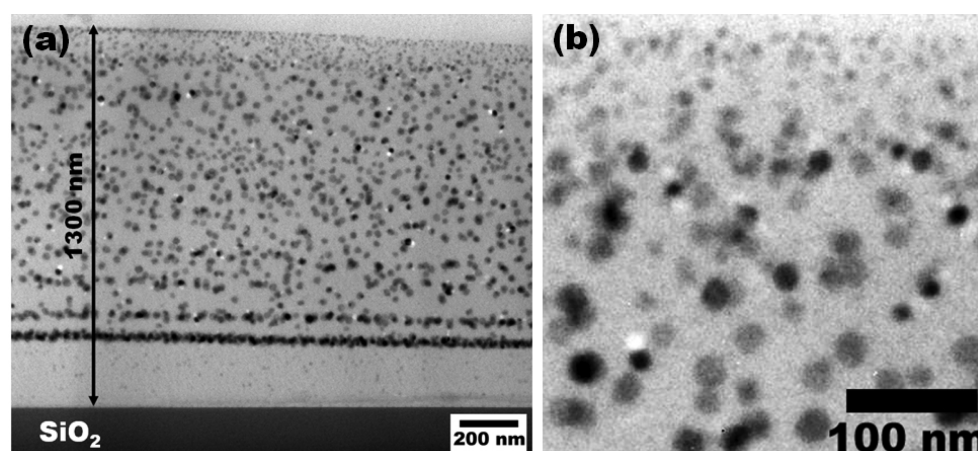


Fig. 2. Cross-sectional TEM images of Cu-Based nanoparticles in multiple-stacked PI films cured at 350°C for 2 h with a 1000 sccm N₂ gas flow rate: (a) entire 1300 nm thick image and (b) a magnified image of the nanoparticles.

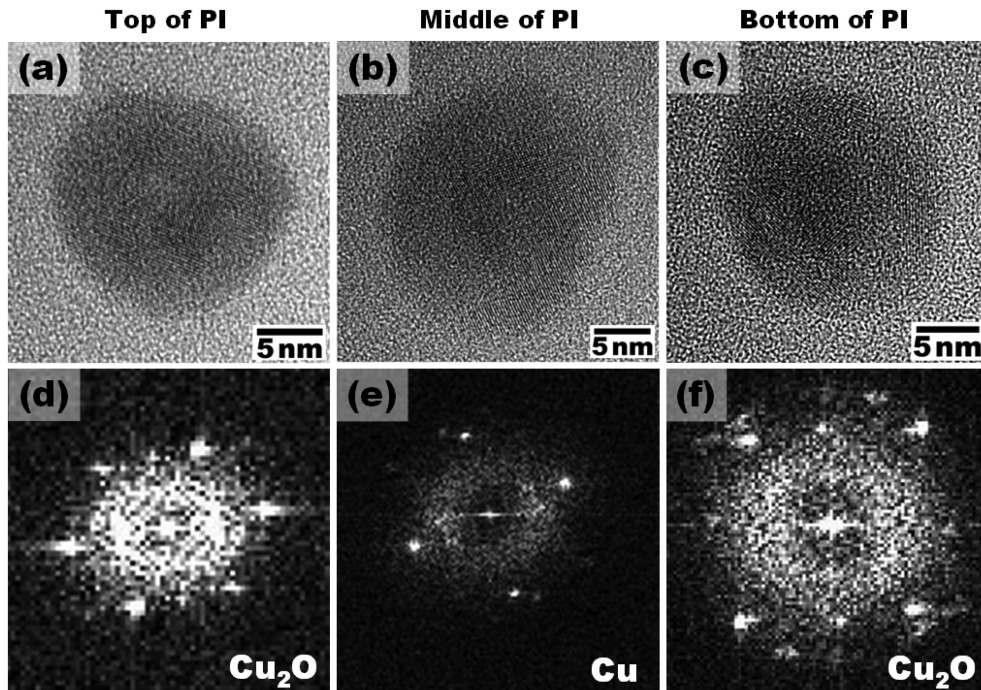


Fig. 3. High-resolution TEM images and the corresponding Fourier transformation images of Cu-based nanoparticles in multiple-stacked PI film cured at 350°C for 2 h in a 100 sccm N₂ gas flow rate: (a) and (d) the top area of the PI film; (b) and (e) the middle area of the PI film; and (c) and (f) the bottom area of the PI film.

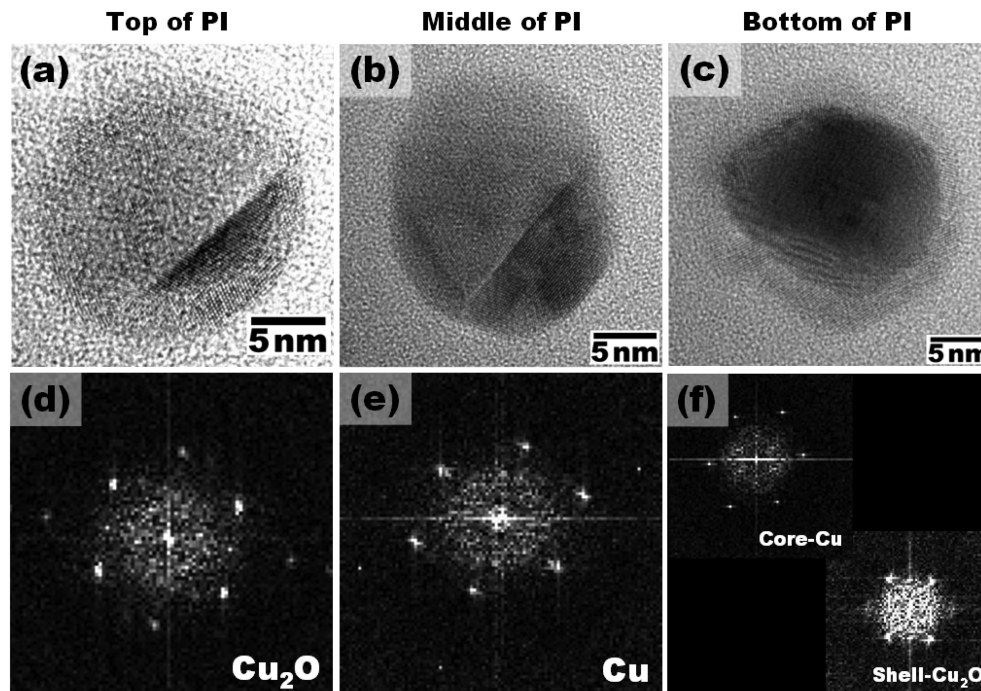


Fig. 4. High-resolution TEM images and corresponding Fourier transformation images of Cu-based nanoparticles in multiple-stacked PI film cured at 350°C for 2 h in a 1000 sccm N₂ gas flow rate: (a) and (d) the top area of the PI film; (b) and (e) the middle area of the PI film; and (c) and (f) the bottom area of the PI film.

relation to their positions. For references, we compared our HRTEM results with those of Urban.^[8,9] In the sample cured at a 100 sccm gas flow rate, the nanoparticles in the PI film

were identified as cuprous oxide (Cu₂O) [110] in the top region, Cu [001] in the middle region, and Cu₂O [001] in the bottom region. In the sample cured at a 1000 sccm gas flow

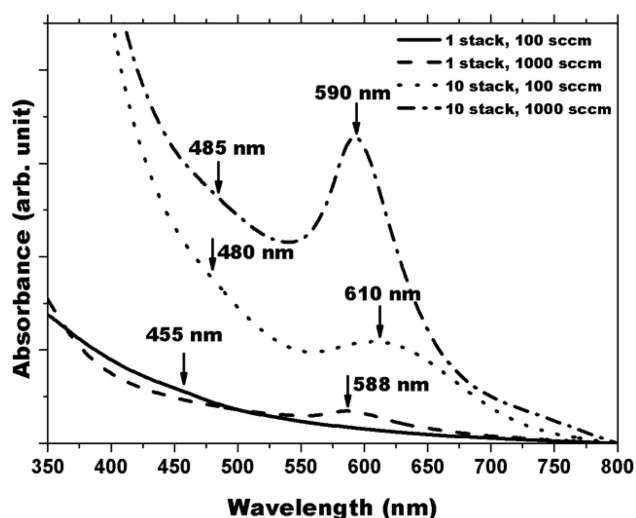


Fig. 5. Optical absorption properties of the multiple-stacked PI films containing nanoparticles.

rate, the phases of nanoparticles in the PI film were identified as Cu_2O [110] in the top region and Cu [110] in the middle region. In the bottom region, we observed core-shell structured nanoparticles and identified the core and shell as Cu [110] and Cu_2O [111], respectively.

Figure 5 shows the ultraviolet-visible (UV-vis) absorption properties of multiple-stacked PI films. Two different absorption peaks were observed in thick PI samples from the multiple-stacking method: one peak, observed near 480 nm, seems to have originated from the quantum confinement effect of Cu_2O nanoparticles;^[13] the other peak, observed near 600 nm, could be the SPR peak of metallic Cu nanoparticles.^[14] The optical absorption intensities in the 10-layer stacked samples are more strongly enhanced than those in the single-stacked samples. The absorption intensity of the sample is controllable via the number of stacks.

The TEM and optical analysis results show the difference between single-stacked thin samples and multiple-stacked thick samples. In a previous study, the Cu or Cu_2O nanoparticles in 100 nm thick PI films were selectively formed in relation to the gas flow rate (1000 sccm or 100 sccm) during the thermal curing.^[14] The HRTEM results confirm that Cu_2O and Cu-phase nanoparticles coexist in thick PI films cured at 100 sccm or 1000 sccm. The UV-vis spectroscopy absorption results confirm that thin PI film and thick PI film have different ways of forming nanoparticles. From these results, we can deduce that the gas flow effect in multiple-stacked thick PI samples differs from the gas flow effect in single-stacked thin PI samples. When nanoparticles are far from the

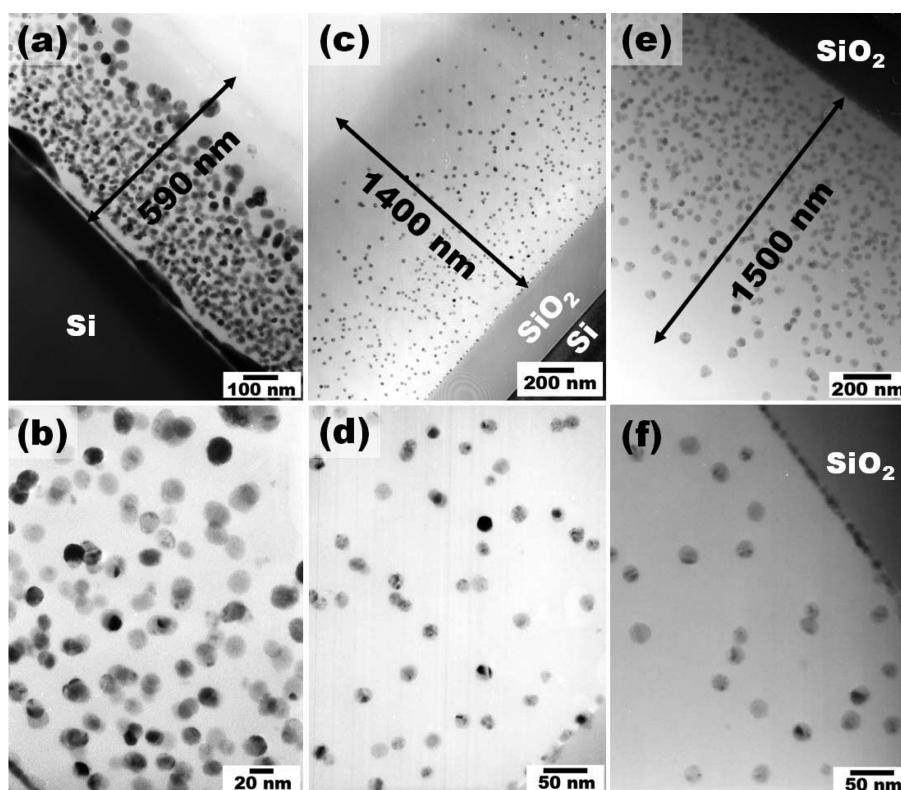


Fig. 6. Cross-sectional TEM images of Cu-based nanoparticles in PI films cured at 350°C for 2 h in a nitrogen atmosphere: (a) and (b) 7.5 wt% PAA/Cu 25 nm/Si; (c) and (d) 10 wt% PAA/Cu 10 nm/SiO₂; (e) and (f) 10 wt% PAA/Cu 25 nm/SiO₂; (note that (c), (d), (e), and (f) are reproduced from^[17]).

PI film surface in thick samples, the gas flow effect has negligible influence on the formation of nanoparticles.

4. CONCENTRATED PAA METHOD

Figure 6 shows cross-sectional TEM images of the PI thick films that contain nanoparticles fabricated with concentrated PAA. The thickness of PI films fabricated by using 7.5 wt% PAA and 10 wt% PAA with evaporated 25 nm thick Cu thin films is shown in Figs. 6(a) and 6(e), respectively. The 7.5 wt% PAA specimen forms a PI film with a thickness of about 590 nm and an observable residual Cu thin film. In contrast, there is no residual Cu thin film in the 1500 nm thick PI film fabricated with a 10 wt% PAA solution. Because one unit of PAA can dissolve two Cu atoms,^[12] more metal atoms react with higher concentrated PAA. To optimize the concentration of the PAA and the spin-coating condition, we control the thickness of the PI film that contains nanoparticles.

In Figs. 6(c) and 6(e), we can observe a difference in the amount of fabricated nanoparticles in the PI films fabricated with evaporated 10 nm thick and 25 nm thick Cu thin films with 10 wt% PAA. In both cases, the nanoparticles are dispersed and have a circular shape. At the interface of the PI film and SiO₂, the nanoparticles are in contact with the SiO₂ surface and this type of contact reduces the surface energy. The nanoparticles of the 10 wt% PAA/evaporated 10 nm thick Cu sample have a diameter of about 18 nm to 20 nm, whereas the nanoparticles of the 10 wt% PAA/evaporated 25 nm thick Cu sample have a diameter of about 28 nm to 30 nm. As the density of reacted Cu increases, the Cu atoms can be agglomerated and the size of the precipitated nanoparticles increases. The amount of nanoparticles in the PI film

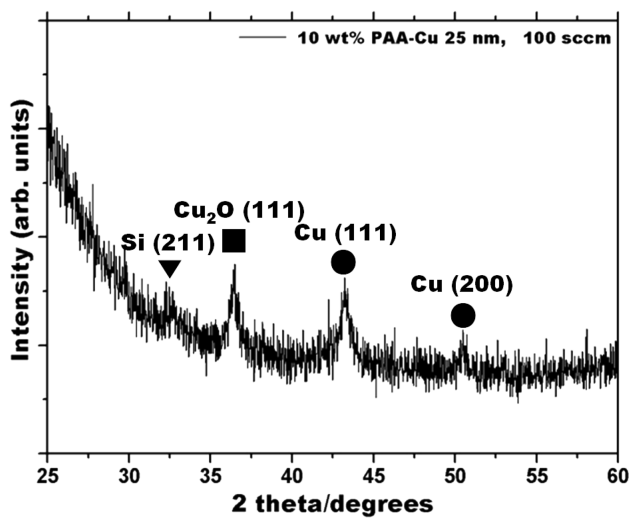


Fig. 7. XRD results of a 10 wt% PAA/25 nm Cu/SiO₂ specimen cured at 350°C for 2 h in a 100 sccm nitrogen gas flow rate (reproduced from^[17]).

can be controlled by changing the thickness of the deposited Cu thin film.

To identify the phase of nanoparticles in the PI films fabricated with the concentrated PAA, we took XRD measurements and the results, which are shown in Fig. 7, reveal that the nanoparticles consist of Cu and Cu₂O phases in a thick PI film. These results are similar to those of the multiple-stacking method. The gas flow effect in thick PI films is not the same as that in thin PI films.

Figure 8 shows the optical absorption peaks in relation to the thickness of fully reacted Cu thin films and the concentration of PAA. The 10 wt% PAA samples cured at a 100 sccm gas flow rate and the 2.5 wt% PAA sample cured at a 1000 sccm gas flow rate have the same SPR absorption peak position of Cu nanoparticles at around 588 nm. However, the 10 wt% PAA samples have no blue-shifted absorption peak from the Cu₂O nanoparticles at around 470 nm due to the

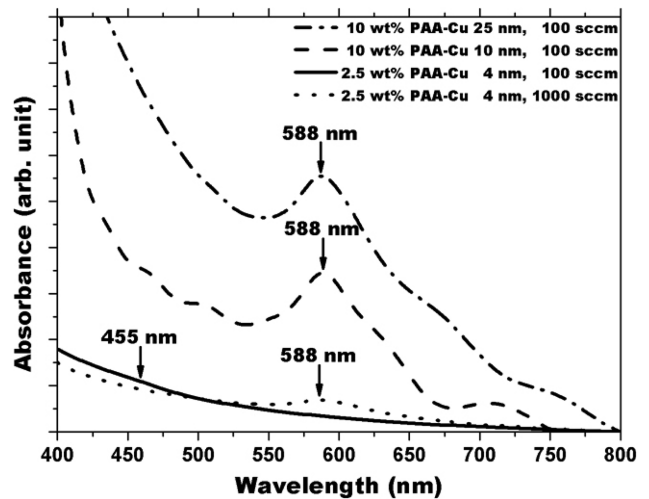


Fig. 8. Optical absorption properties of PI films containing nanoparticles fabricated with the PAA (10 wt% or 2.5 wt%) and Cu thin films (4 nm, 10 nm, or 25 nm).

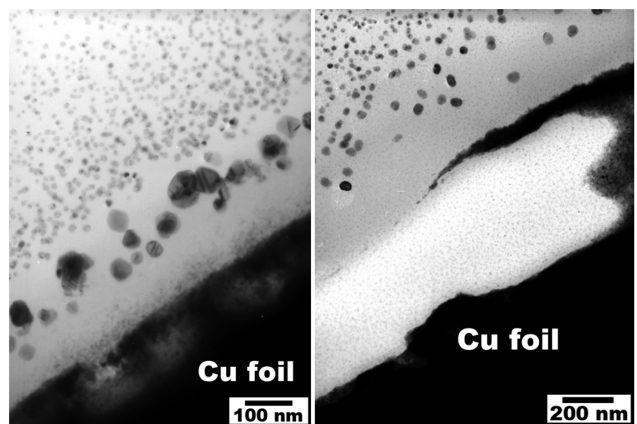


Fig. 9. The fabricated nanoparticles from the reaction between Cu foil and 10 wt% PAA.

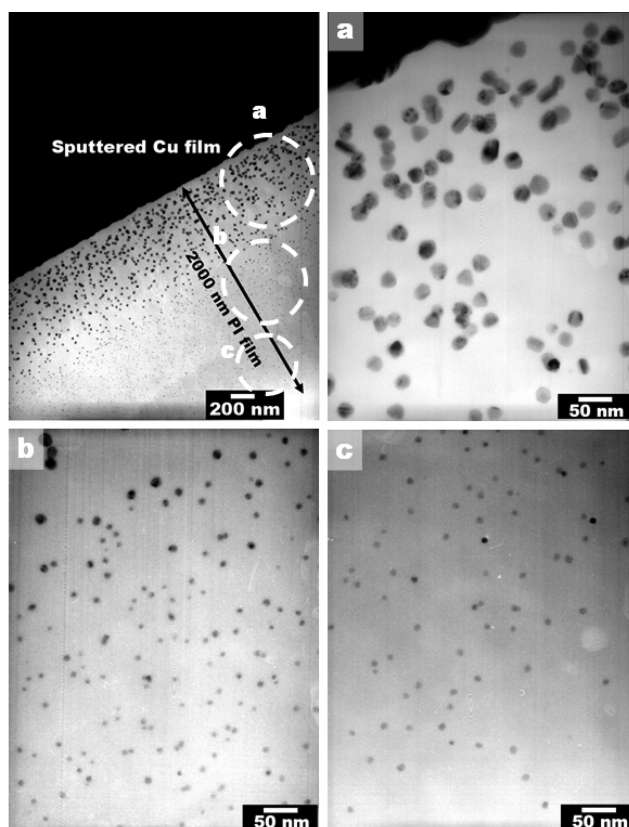


Fig. 10. The fabricated nanoparticles from the reaction between the 0.5 μm thick sputtered Cu and 10 wt% PAA.

constructive peaks from the PI's own thickness, whereas the 2.5 wt% PAA sample clearly has a blue-shifted absorption peak.^[13] In the case of the SPR absorption peak from the Cu nanoparticles, the intensity of the optical property is controlled through the amount of deposited Cu thin film and the concentrations of PAA. When Cu thin films are fully reacted with PAA, the intensity of the SPR absorption is enhanced by the increased thickness of the Cu thin films.

To observe the nanoparticle formation from the unlimited metal sources, we prepared two samples: a Cu foil sample and a 0.5 μm thick sputtered Cu/50 nm thick Ti/SiO₂ sample. The Cu foil had been etched to remove the native-oxide layer on the surface. The 10 wt% PAA was spin-coated on the etched Cu foil and sputtered Cu thin film and then thermally cured under the same conditions as before. Figure 9 shows TEM images of the fabricated particles in the PI film. Although very big particles of 50 nm to 80 nm are observed near the Cu interface, most of the fabricated nanoparticles have the size between 11 nm and 22 nm. The bigger particles are formed in the high concentrated region because the region near the Cu interface has a high Cu ion concentration. Figure 10 shows the nanoparticles in the 2000 nm thick PI film that formed when the 10 wt% PAA reacted with the sputtered Cu sample. The nanoparticles varied in size from 8

nm to 28 nm, depending on their positions in the thick PI film. As the nanoparticles are far from the boundary of the sputtered Cu thin film, the size and density of the nanoparticles are decreased due to the lower concentration of Cu; note also that the Cu ions have a limited diffusion path from the Cu thin film. The results from the Cu foil and sputtered Cu specimens reveal that the particle size is sensitive to the Cu concentration in the PAA films.

5. SUMMARY

We successfully demonstrated the fabrication of Cu-based nanoparticles in thick PI films via two different methods of fabrication: the multiple-stacking method and the concentrated PAA method. The multiple-stacking method can precisely control the entire thickness of film and the distance between the arrays of nanoparticles. However, there are many obstacles to overcome when fabricating nanoparticles with a controlled size. As the number of stackings is increased, the additional processing time of the fabrication causes high costs, and it is possible that the film can be contaminated during the stacking-process. The concentrated PAA method is a simple fabrication process. When we optimize the concentration of the PAA and the spin-coating condition, we can easily control at will the thickness and properties of PI film that contains nanoparticles.^[9,10] In addition, we can control the size of the fabricated nanoparticles through the amount of reacted metal.

In both cases, we observed that spherical nanoparticles were dispersed throughout the entire thick PI film. The density and optical absorption property of the fabricated nanoparticles were successfully controlled in both methods. Although the samples were cured at a 100 sccm or 1000 sccm gas flow rate of high purity nitrogen, the XRD and HRTEM studies reveal that Cu and Cu₂O nanoparticles were formed together in the thick PI films in both fabrication methods; in contrast, the phase of nanoparticles in the thin PI films (about 100 nm) was selectively formed as Cu or Cu₂O via the gas flow control during thermal curing. Further study is needed to understand the effect of the gas flow.

ACKNOWLEDGEMENT

This research was supported by a grant (code #: 08K1501-02410) from the Center for Nanostructured Materials Technology under the 21st Century Frontier R&D Programs of the Ministry of Education, Science, and Technology, Korea.

REFERENCES

1. A. P. Alivisatos, *J. Phys. Chem.* **100**, 133226 (1996).
2. M. Gao, C. Lesser, S. Kirstein, J. Mohwald, A. L. Rogach, and H. Weller, *J. Appl. Phys.* **87**, 2297 (2000).

3. M. T. Harrison, S. V. Kershaw, M. G. Burt, A. L. Rogach, A. Kornowski, A. Eychmuller, and H. Weller, *Pure Appl. Chem.* **72**, 295 (2000).
4. R. Abargues, J. Marqués-Hueso, J. Canet-Ferrer, E. Pedruza, J. L. Valdés, E. Jiménez, and J. P. Martinez-Pastor, *Nanotechnology* **19**, 355308 (2008).
5. S. Kim, *Electron. Mater. Lett.* **3**, 109 (2007).
6. M. M. Sung, *Electron. Mater. Lett.* **3**, 137 (2007).
7. Y. Chung, H. P. Park, H. J. Jeon, C. S. Yoon, S. K. Lim, and Y.-H. Kim, *J. Vac. Sci. Technol. B* **21**, L9 (2003).
8. S. K. Lim, K. J. Chung, C. K. Kim, D. W. Shin, Y.-H. Kim, and C. S. Yoon, *J. Appl. Phys.* **98**, 084309 (2005).
9. G. Simone, G. Perozziello, V. Tagliaferri, and N. Szita, *Mater. Res. Soc. Symp. Proc.* **951**, 0951-E03-23 (2007).
10. D. Zimnitsky, C. Jiang, J. Xu, Z. Lin, and V. V. Tsukruk, *Langmuir* **23**, 4509 (2007).
11. J. Urban, H. Sack-Kongehl, K. Weiss, I. Lisiecki, and M.-P. Pileni, *Cryst. Res. Technol.* **35**, 731 (2000).
12. J. Urban, *Cryst. Res. Technol.* **33**, 1009 (1998).
13. K. Borgohain, N. Murase, and S. Mahamuni, *J. Appl. Phys.* **92**, 1292 (2002).
14. J.-Y. Choi, W. Dong, and Y.-H. Kim, *Colloids and Surface A: Physicochem, Eng. Aspects* **313**, 335 (2008).
15. Y.-H. Kim, *Electron. Mater. Lett.* **2**, 1 (2006).
16. J.-Y. Choi, W. Dong, D. J. Choi, and Y.-H. Kim, *J. Nanosci. Nanotechnol.* **8**, 1 (2008).
17. J.-R. Yoon, D. J. Choi, D.-H. Oh, T. W. Kim, and Y.-H. Kim, *J. Nanosci. Nanotechnol.* **8**, 1 (2008).